Full length article

Stability analysis of shallow tunnels subjected to eccentric loads by a boundary element method

Mehdi Panji [a,*], Hamid Koohsari [a], Mohammad Adampira [b], Hamid Alielahi [a], Jafar Asgari Marnani [c]

[a] Department of Civil Engineering, Zanjan Branch, Islamic Azad University, Zanjan, Iran
[b] Department of Civil Engineering, Science and Research Branch, Islamic Azad University, Tehran, Iran
[c] Department of Civil Engineering, Technical and Engineering Faculty, Central Tehran Branch, Islamic Azad University, Tehran, Iran

ABSTRACT

In this paper, stress behavior of shallow tunnels under simultaneous non-uniform surface traction and symmetric gravity loading was studied using a direct boundary element method (BEM). The existing full-plane elastostatic fundamental solutions to displacement and stress fields were used and implemented in a developed algorithm. The cross-section of the tunnel was considered in circular, square, and horseshoe shapes and the lateral coefficient of the domain was assumed as unit quantity. Double-node procedure of the BEM was applied at the corners to improve the model including sudden traction changes. The results showed that the method used was a powerful tool for modeling underground openings under various external as well as internal loads. Eccentric loads significantly influenced the stress pattern of the surrounding tunnel. The achievements can be practically used in completing and modifying regulations for stability investigation of shallow tunnels.

1. Introduction

Along with the population growth, tunnel excavation and sub-surface openings have become a major requirement for urban transportation, especially in big cities. Tunnels should be designed in such a way that could be sufficiently powered against static and dynamic loads. On the other hand, urban tunnels that are mainly close to the ground surface in urban areas can affect the behavior of the existing structures such as buildings, roads and railways. Therefore, it is necessary for engineers to utilize appropriate tools as well as efficient methods to determine more precise ground responses.

Technically speaking, there are several studies on stability analysis of shallow tunnels. Stability of circular tunnels has been extensively studied at Cambridge since the 1970s, for example, the works reported by Atkinson and Cairncross (1973), Cairncross (1973), Mair (1979), Seneviratne (1979), and Davis et al. (1980). Before the 1990s, most of the published works have focused on the stability of circular

tunnel in undrained clayey soil. Later, theoretical solutions for circular tunnel problems in drained conditions have been determined by Muhlhaus (1985) and Leca and Dormieux (1990). Recently, using the theoretical approach proposed by Fraldi and Guarracino (2009), they presented a full analytical solution for collapse mechanisms of tunnels with arbitrary excavation profiles based on plastic Hoek–Brown criterion (Fraldi and Guarracino, 2010).

In recent decades, a large number of numerical methods have been proposed to calculate the responses of underground structures and estimate failure of surrounding rock mass. Among these methods are finite element method (FEM) and finite difference method (FDM). Rowe and Kack (1983) predicted soft ground settlement located above the tunnel using FEM. In order to model the tunnel geometry and determine the failure mechanisms, FEM was used by Koutsabeloulis and Griffiths (1989). Lee and Rowe (1991) calculated the deformations that occur in clayey soil surrounding the tunnel by three-dimensional (3D) FEM. Jao and Wang (1998) performed an extensive study on various soils in terms of the stability of shallow foundations located on underground tunnels. They simulated soil models and used FEM to investigate the effect of different tunnel positions. To investigate the behavior of unconsolidated soils with inclined layers, Park and Adachi (2002) applied an experimental procedure as well as finite element (FE) analysis.

Azevedo et al. (2002) evaluated the response of residual soils in the presence of shallow tunnels using elastoplastic FE back analysis and found a good agreement between the displacements obtained from field studies and numerical results.

The application of FE limit analysis to the undrained stability of shallow tunnels was first considered by Sloan and Assadi (1993). They investigated the case of a plane-strain circular tunnel using linear programming techniques in cohesive soil whose shear strength varied linearly with depth. Later, Lyamin and Sloan (2000) considered the stability of a plane-strain circular tunnel in a cohesive-frictional soil using a developed nonlinear programming technique. Yamamoto et al. (2011a, b, 2012, 2013) investigated the stability of plane-strain single/dual circular as well as square tunnels in cohesive-frictional soils subjected to surcharge loading using FE limit analysis technique. They found that the failure mechanisms of shallow square tunnels were completely different from those of shallow circular tunnels due to the absence of curved geometries. Fraldi and Guarracino (2011) carried out a comparative study between numerical and analytical approaches for modeling plastic collapse in circular tunnels. They indicated that the numerical modeling of the evolution of progressive failure leading to collapse in the tunnels remains a complicated issue, which requires great care in preparing the model and analyzing the results.

Despite the simple formulation and also development in elastoplastic problems, FEM and FDM are continually accompanied by a large volume of calculations for analyzing problems including unlimited boundaries. Therefore, data and computation time are subsequently increased. Also, by applying approximate boundary conditions to truncated boundaries, the models become complicated and the accuracy is reduced. On the other hand, the boundary element method (BEM) can be practically used for the problems in which the domain includes infinite as well as semi-infinite boundaries because of discretizing boundaries instead of domain. It is worth mentioning that full-plane BEM has been completely developed for linear elastostatic problems (Brebbia and Dominguez, 1989).

Although the BEM has been formed over four decades, qualitative improvements of computers in recent decades have accelerated the development of BEM as well as other engineering issues. For the first time, boundary discretizing was used in 1903 for the potential flow equations (Fredholm, 1903). After a few decades, many researchers developed boundary integral equations (BIEs) to solid mechanics (Massonnet, 1965; Benjumea and Sikarskie, 1972; Banerjee and Driscoll, 1976). Since 1980, BEM has been also used for solving rock/soil mechanics problems and some researchers have used it for studying opening models in the continuous infinite space (Banerjee and Butterfield, 1981; Crouch and Starfield, 1983). During the same period, between 1980 and 1983, Hoek and Brown presented a criterion called the Hoek–Brown failure criterion for the intact/fractured rock resistance, whose complete version was presented in 1992 (Hoek and Marions, 2007). Commercial softwares, such as FLAC[2D] and EXAMINE[2D], which have been used by some researchers for modeling two-dimensional (2D) underground structures, could not create the foundation shallow loads (Shah, 1992; Martin et al., 1999; Kooi and Verruijt, 2001). Panji (2007), Asgari Marnani and Panji (2007, 2008), and Panji et al. (2011, 2012, 2013) have recently prepared an algorithm based on full/half-plane elastostatic fundamental solutions of direct BEM and used it to analyze geotechnical structures with different cases of effective loads.

The literature review showed that the presence of shallow foundations on underground tunnels could cause the interaction of the induced stresses by shallow loads with tunnels, which reduces stability as well as bearing capacity (Banerjee and Driscoll, 1976; Panji et al., 2012). In previous studies, tunnels with in-situ loads have been only considered. Therefore, the purpose of the present study was to observe the behavior of shallow tunnels including different cross-sections subjected to various simultaneous gravity and shallow loadings. In this regard, the effect of one of the key parameters, i.e. the eccentricity of shallow loads, was studied by a developed algorithm based on full-plane elastostatic BEM.

2. Full-plane BEM

After applying the weighted residual integral to Navier's elastostatic equilibrium equation, regardless of body forces, the following equation can be obtained (Brebbia and Dominguez, 1989):

$$\int_{\Omega} \sigma_{kj,j} u_k^* d\Omega = 0 \tag{1}$$

where u_k^* is the weight function or Kelvin's fundamental solution for full-plane, Ω indicates the domain, and $\sigma_{kj,j}$ is the stress component. After twice integration by parts of Eq. (1), Green's equation is obtained as follows:

$$\int_{\Omega} \sigma_{kj,j}^* u_k d\Omega = -\int_{\Gamma} p_k u_k^* d\Gamma + \int_{\Gamma} u_k p_k^* d\Gamma \tag{2}$$

where p_k and u_k indicate the stress and boundary displacements, respectively; p_k^* is the full-plane stress fundamental solution; and Γ specifies the boundary. Using the Dirac delta method, the following BIE is presented after omitting the domain terms:

$$c_{lk}^i u_l^i + \int_{\Gamma} p_{lk}^* u_k d\Gamma = \int_{\Gamma} u_{lk}^* p_k d\Gamma \tag{3}$$

where $c_{lk}^i = 1 - \theta_i/(2\pi)$, θ_i is the boundary fraction angle of node i; u_{lk}^* and p_{lk}^* are the full-plane displacement and traction fundamental solution, respectively (Brebbia and Dominguez, 1989). After solving Eq. (3), boundary unknowns including displacements as well as tractions can be obtained for each boundary node i. It is noteworthy that in order to determine stresses at any defined point within the domain, full-plane stress fundamental solutions can be obtained using the displacement fields as follows:

$$\sigma_{ij} = \int_{\Gamma} D_{kij}^* p_k d\Gamma - \int_{\Gamma} S_{kij}^* u_k d\Gamma \tag{4}$$

where D_{kij}^* and S_{kij}^* are the internal stress fundamental solutions which can be found in Brebbia and Dominguez (1989).
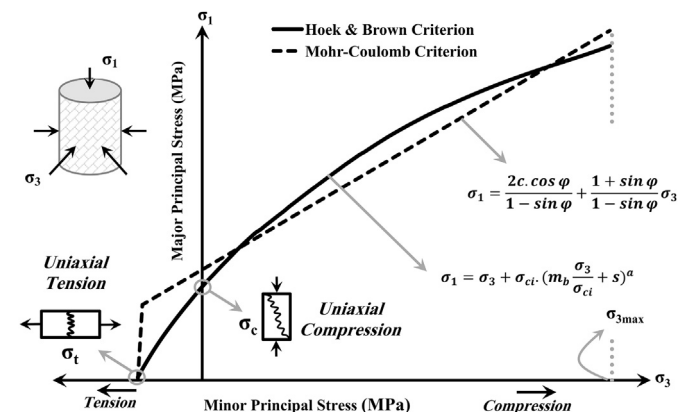

Fig. 1. Relationship between maximum/minimum principal stresses of Hoek–Brown criterion and equivalent values obtained using Mohr–Coulomb criterion.

Table 1
Rock mass properties obtained from RocLab software.

Hoek–Brown classification					Hoek–Brown criterion		
σ_{ci} (MPa)	GSI	M_i	D	E_i (GPa)	m_b	s	a
60	50	16	0	70	2.68284	0.003866	0.505734
Mohr–Coulomb fit		Failure envelope range			Rock mass parameters		
c (MPa)	φ (°)	Application	σ_{3max} (MPa)	Unit weight (kN/m³)	Tunnel depth (m)	σ_t (MPa)	σ_c (MPa)	σ_{cm} (MPa)
0.552333	58	Tunnels	0.701873	26	50	−0.08646	3.61363	13.1089

Fig. 2. Discretized model using full-plane BEM.

3. Rock mass strength

One of the important issues in the design of underground space where tunnel is excavated is the strength of rock mass. In the present paper, in order to determine the rock mass strength, RocLab V.4 software was applied. This software has been established based on the Hoek–Brown failure criterion, the developed form of which is as follows (Hoek et al., 2002):

$$\sigma_1 = \sigma_3 + \sigma_{ci}\left(m_b\frac{\sigma_3}{\sigma_{ci}} + s\right)^a \tag{5}$$

where σ_1 is the maximum principal stress, σ_3 is the minimum principal stress (confining stress), σ_{ci} is the uniaxial compressive strength of intact rock, m_b is a constant depending on in-situ rock mass properties, and s and a are the coefficients depending on the joint state of the rock mass. Assuming $\sigma_3 = 0$ in Eq. (5), the reduced uniaxial compressive strength of rock was obtained as follows:

$$\sigma_c = \sigma_{ci}s^a \tag{6}$$

Similarly, by considering $\sigma_1 = 0$ in Eq. (5) and solving it in terms of σ_3, uniaxial tensile strength of the rock was achieved. Hoek (1983) showed that the uniaxial tensile strength of the rock was the same as the bi-axial tensile strength of brittle rocks. Assuming $\sigma_1 = \sigma_3 = \sigma_t$, the tensile strength of rock mass would be as follows:

$$\sigma_t = \frac{-s\sigma_{ci}}{m_b} \tag{7}$$

Hoek–Brown relation is graphically shown in Fig. 1. Eqs. (6) and (7) demonstrate that the Hoek–Brown curve intersects with the maximum and minimum principal stress curves, respectively. After

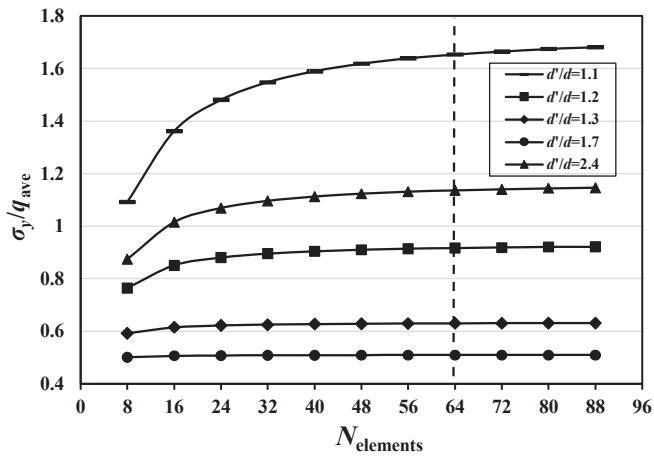**Fig. 3.** Discretized model using full-plane BEM in the surrounding zone of square tunnel.

Fig. 4. Convergence in the number of elements in square tunnel.

determining the rock mass strength, strength coefficient (ratio of strength to the obtained stress value), which is very important in design procedures, can be defined. Rock characteristics are given in Table 1, including Hoek–Brown classification, Hoek–Brown criterion, Mohr–Coulomb fit, failure envelope range and rock mass parameters. Parameters of these characteristics were previously defined. It is noteworthy that all the analyses were based on dolerite rock properties in the present study.

4. Numerical modeling

To prepare the model and carry out the analyses, an algorithm was developed based on the above formulation by MATLAB programming language (Brebbia and Dominguez, 1989; Asgari Marnani and Panji, 2008). This software includes six main subroutines; it first receives input values from quadratic discretized model, analyzes them, and obtains the results including displacements as well as stresses. Then, using the tensile/compressive strength of the rock mass obtained from RocLab software and considering a safety factor for the given cross-section, the failure radius is determined.
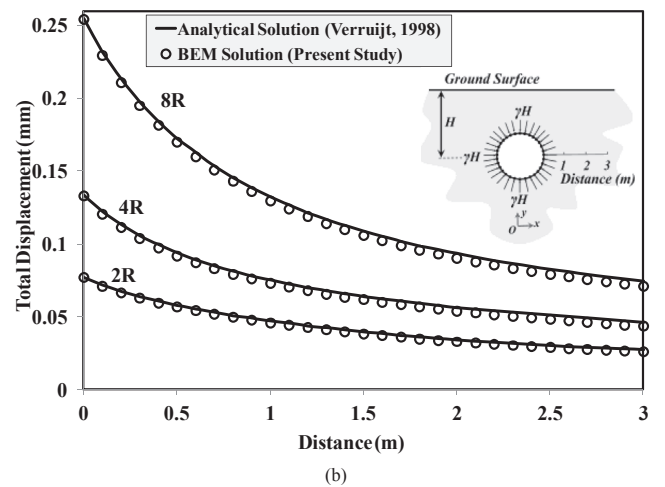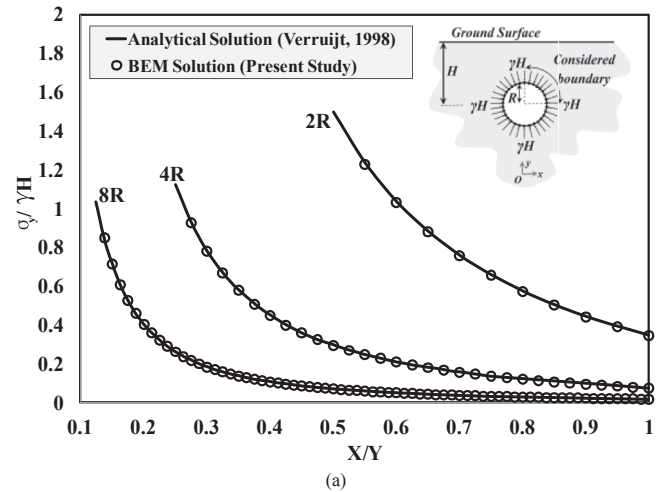

(a)

(b)

Fig. 6. Comparison of BEM results with the analytical responses (Verruijt, 1998) for uniform/triangular loads. (a) Vertical stresses at different distances from the wall of tunnel under gravity loads at depths of $2R$, $4R$ and $8R$. (b) Total displacements at different distances from the wall of the tunnel under gravity loads at depths of $2R$, $4R$ and $8R$.

Fig. 5. Comparison of the analytical (Poulos and Davis, 1974) and BEM results (the present study) for vertical stress on the tunnel boundary at depths of $2R$, $4R$ and $8R$ under uniform/triangular loads.
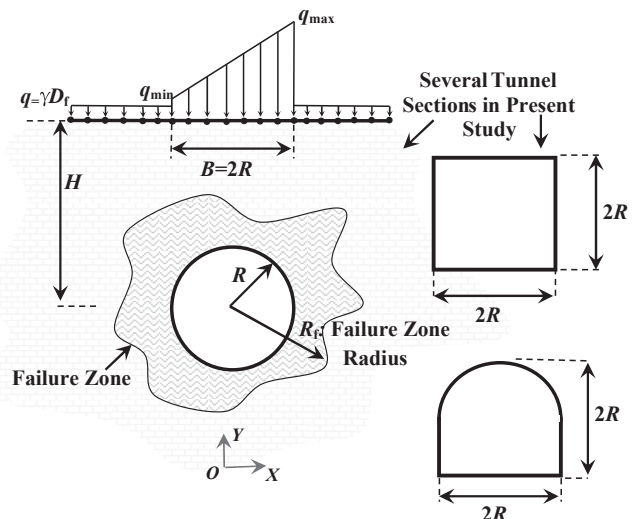

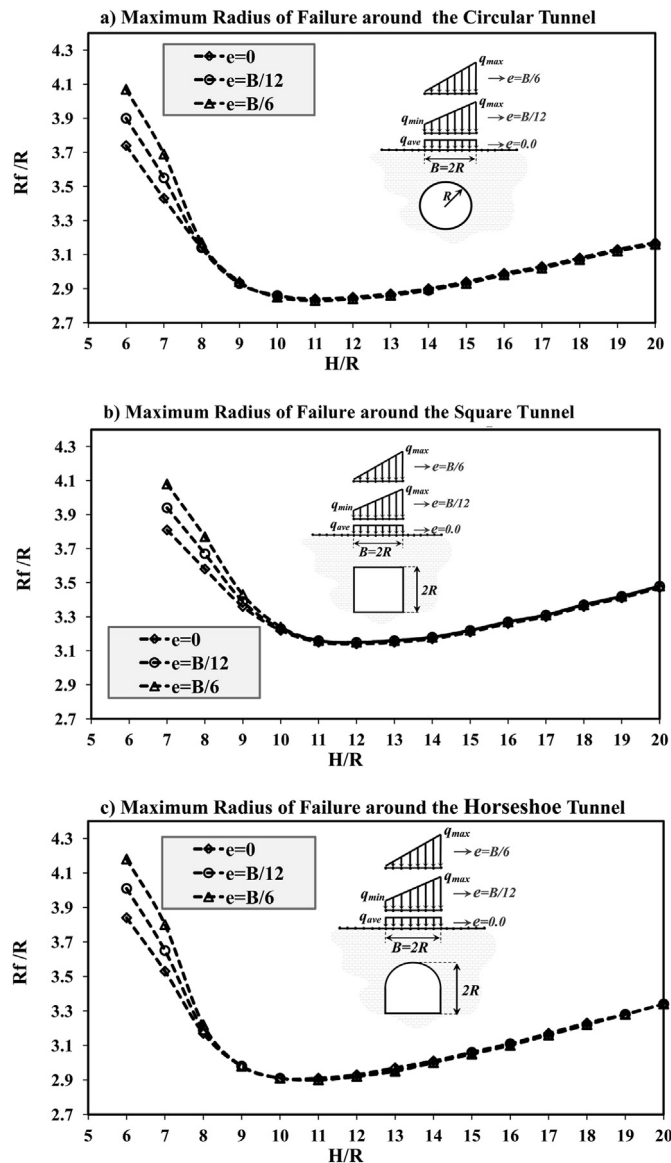**Fig. 7.** Tunnel cross-sections for studying failure radius.

Fig. 8. Failure propagation for tunnels with different sections and eccentricities versus the buried depth by assuming a fixed loading width ($B = 2R$) and a unit safety factor.

4.1. Assumptions

The following assumptions are made in this paper:

(1) Due to the approximately linear behavior of dolerite rock, soil material was assumed to be composed of this rock type with the Poisson's ratio of 0.15, elasticity modulus of 70 GPa, and density of 2850 kg/m^3.
(2) Soil lateral pressure coefficient was assumed to be unit.
(3) Circular, horseshoe, and square sections were used for the tunnel.
(4) All length parameters were presented in terms of tunnel radius R.
(5) When the collocation point (source) was in the integration element, to avoid singularity and increase the accuracy of the integration, a special logarithmic numerical quadrature was used.
(6) In order to improve modeling in abrupt stress changes in the ground surface, double-node procedure was used at the corners, as shown in Fig. 2.
(7) The model was discretized by 100, 20, and 50 quadratic elements for the smooth ground surface, traction boundary, and surrounding rocks of the circular tunnel, respectively, as shown in Fig. 2.
(8) The average non-uniform linear loading was assumed as $q_{ave} = 200$ kPa and surface loading buried depth (D_f) was equal to the tunnel radius ($D_f = R$).

4.2. Verification

As can be seen in Fig. 2, in order to verify the numerical modeling, the cases of uniform and non-uniform linear loadings with the width of $B = 2R$ were used. To reduce the error in stress components to be less than 0.5%, the zone with $12B$ from each side and $20B$ in the vertical direction was discretized.

The existence of corners in the square and horseshoe cross-sections results in abrupt stress changes in these points. Therefore, to assess the efficiency of the double-node procedure, a convergence analysis was carried out to obtain the number of the required elements for discretizing the boundary. As can be seen in Fig. 3, different points were considered at the corner of square tunnel. Fig. 4 shows the status of their vertical stresses versus the number of boundary elements. The convergence can be approximately obtained in the use of 64 elements for all distances from the
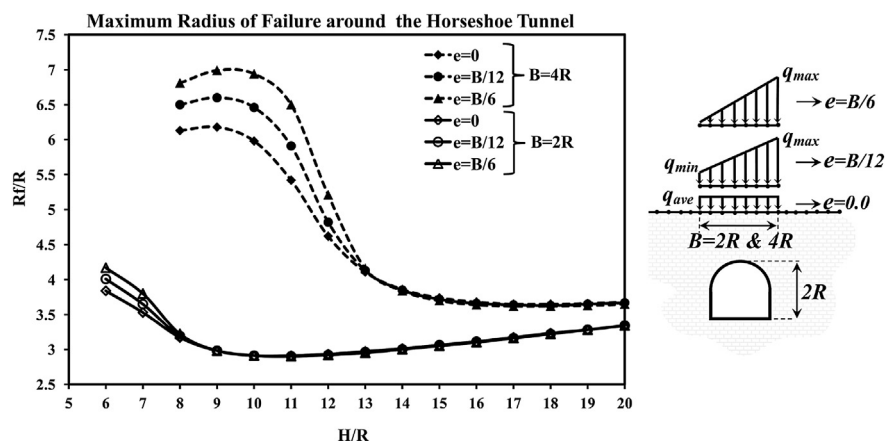

Fig. 9. Failure propagation for tunnel with a horseshoe cross-section versus the buried depth by assuming a unit safety factor.

a) Maximum Radius of Failure around the Tunnels with e=0

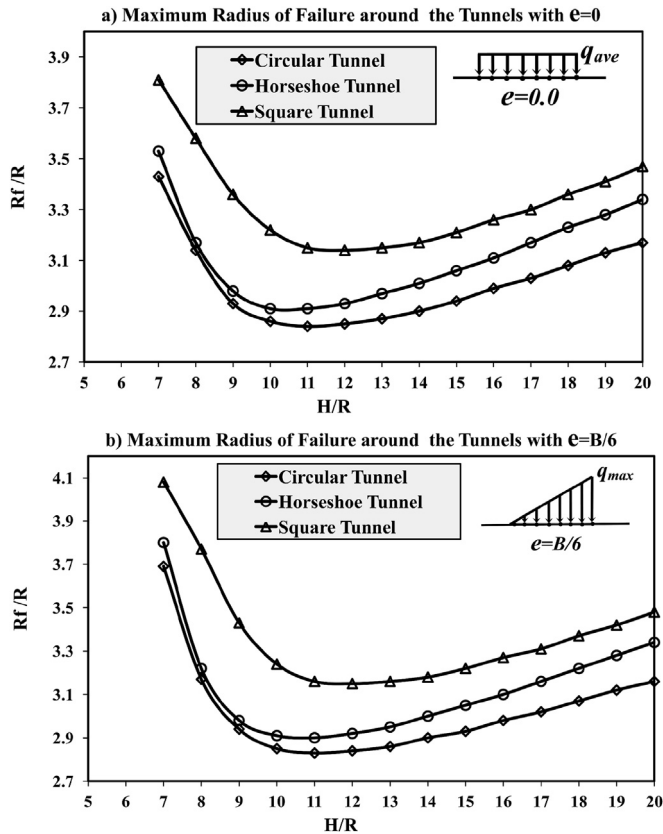### b) Maximum Radius of Failure around the Tunnels with e=B/6

Fig. 10. Distribution of failure radius for various cross-sections of tunnel with the maximum/minimum eccentricity versus the buried depth by assuming a unit safety factor.

corner of the tunnel. Therefore, this value was considered for discretizing the boundary of square and horseshoe cavities as well.

In order to validate the results, as shown in Fig. 2, vertical stresses of the considered points before excavation under uniform and non-uniform loadings were calculated at depths of 2R, 4R, and 8R and compared with the existing analytical solutions (Poulos and
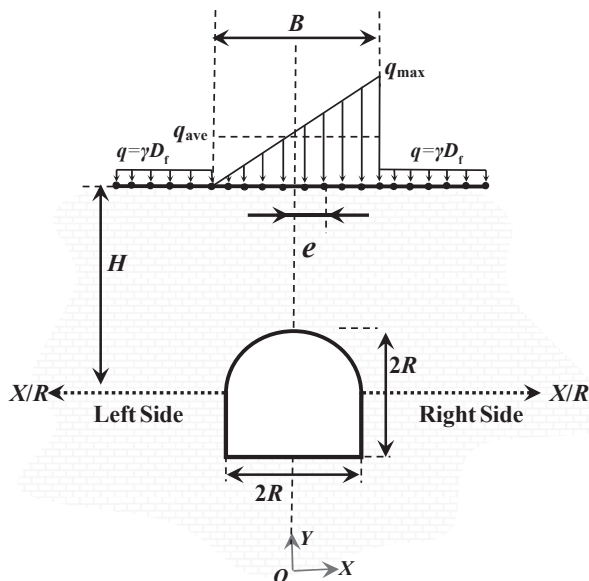

Fig. 11. Schematic view of horseshoe tunnel under non-uniform linear loading with the maximum eccentricity.

Davis, 1974). As can be observed in Fig. 5, favorite accuracy was obtained between the analytical and numerical results for two cases of loading. In the case of gravity pressure (γH), vertical stresses and displacements obtained from BEM were compared with the analytical responses by Verruijt (1998). As can be seen in Fig. 6a, the obtained stress values showed a good agreement with the analytical results. In Fig. 6b, the total displacements were observed at different distances at depths of 2R, 4R, and 8R. As can be observed, the accuracy of the responses was favorite, compared with analytical results.

a) Comparison of the Vertical Stress in Right & Left Sides of Circular Tunnels

b) Comparison of the Vertical Stress in Right & Left Sides of Square Tunnels

c) Comparison of the Vertical Stress in Right & Left Sides of Horseshoe Tunnels
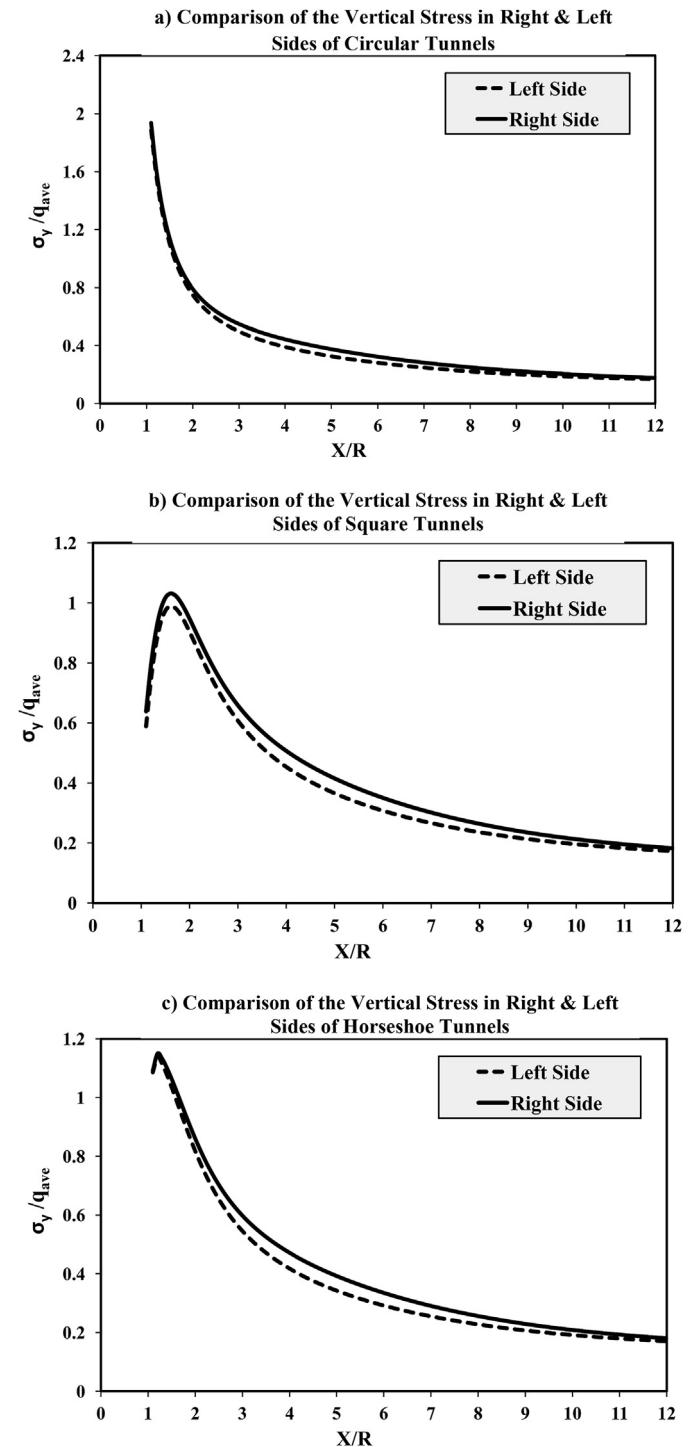

Fig. 12. Vertical stress in horizontal direction of tunnel wall in the left and right sides ($e = B/6$, $H/R = 8$, $D_f = R$, $q_{ave} = 200$ kPa, $B = 4R$).

4.3. Failure zone

Generally, the area around the tunnel, where the ratio of strength to stress (strength coefficient) is less than the safety factor and the stability is controlled by the installation of the support system, is called the failure zone (Martin et al., 1999). In order to determine the failure radius (R_f), as shown in Fig. 7, the effects of shallow loading and its eccentricity were investigated. The results are given in Figs. 8–10. Based on the concepts derived from the elasticity theory, a shallow foundation with the assumed linear traction due to eccentricity (e), away from the formation of negative effects (uplift), has the maximum eccentricity of 1/6 times of its width. Therefore, two values of $e = B/6$ and $e = B/12$ were considered in the present paper.

As can be observed in Fig. 8, each tunnel section with fixed loading width had a certain depth below which the tunnel collapsed. This depth can be defined as the "minimum buried depth". Technically speaking, the existence of tunnel leads to stress development as well as failure zones around it. On the other hand, shallow foundation loading causes the release of stress bubbles from the surface to the depth and consequently creates failure zones. If both the above failure zones occur simultaneously, then a tunnel depth (the minimum buried depth) at which these two zones intersect can be found. This process intensifies the amount of failure stresses, especially at the crown of the tunnel and finally the collapse of tunnel starts. For circular/horseshoe and square tunnels, the minimum buried depth was equal to 6R and 7R, respectively. Also, it can be observed that, by increasing the tunnel's buried depth, the failure radius was decreased due to the reduction of the shallow loading effect and reached its minimum value at a specific point called "optimum buried depth". Then, by increasing the buried depth from this specific value, the failure radius was increased due to the dominance of gravity stress compared with the shallow loading. Therefore, the optimal buried depth of the tunnel, by assuming the constant loading width ($B = 2R$), was equal to 11R and 12R for circular/horseshoe and square tunnels, respectively. As can be seen, by increasing the eccentricity of the shallow loadings, the failure radius of all the three cross-sections was increased. Eccentricity of the shallow loading compared with the loading width was effective until a certain buried depth; afterwards, the effect of eccentricity on the failure radius disappeared. For example, it is clearly observed in Fig. 9 that, in the horseshoe tunnel, the eccentricity effect disappeared at depths of 8R and 13R for the loading widths of 2R and 4R, respectively.

Fig. 10 shows that the failure radius for the horseshoe tunnel is between those of circular and square tunnels. Also, similar behaviors of the horseshoe and circular tunnels appeared at shallow buried depths.

4.4. Loading width (B) effects

In this section, the effects of loading widths (i.e. 1R, 2R, 3R, and 4R) with fixed eccentricity ($e = B/6$) are evaluated. A schematic view of horseshoe tunnel is shown in Fig. 11. In the literature, the vertical stress is higher than horizontal as well as shear stresses either in the crest or in the wall of the tunnel (Panji, 2007; Panji et al., 2011). So, this parameter is considered along the tunnel wall on the left and right sides. The buried depth of shallow loading
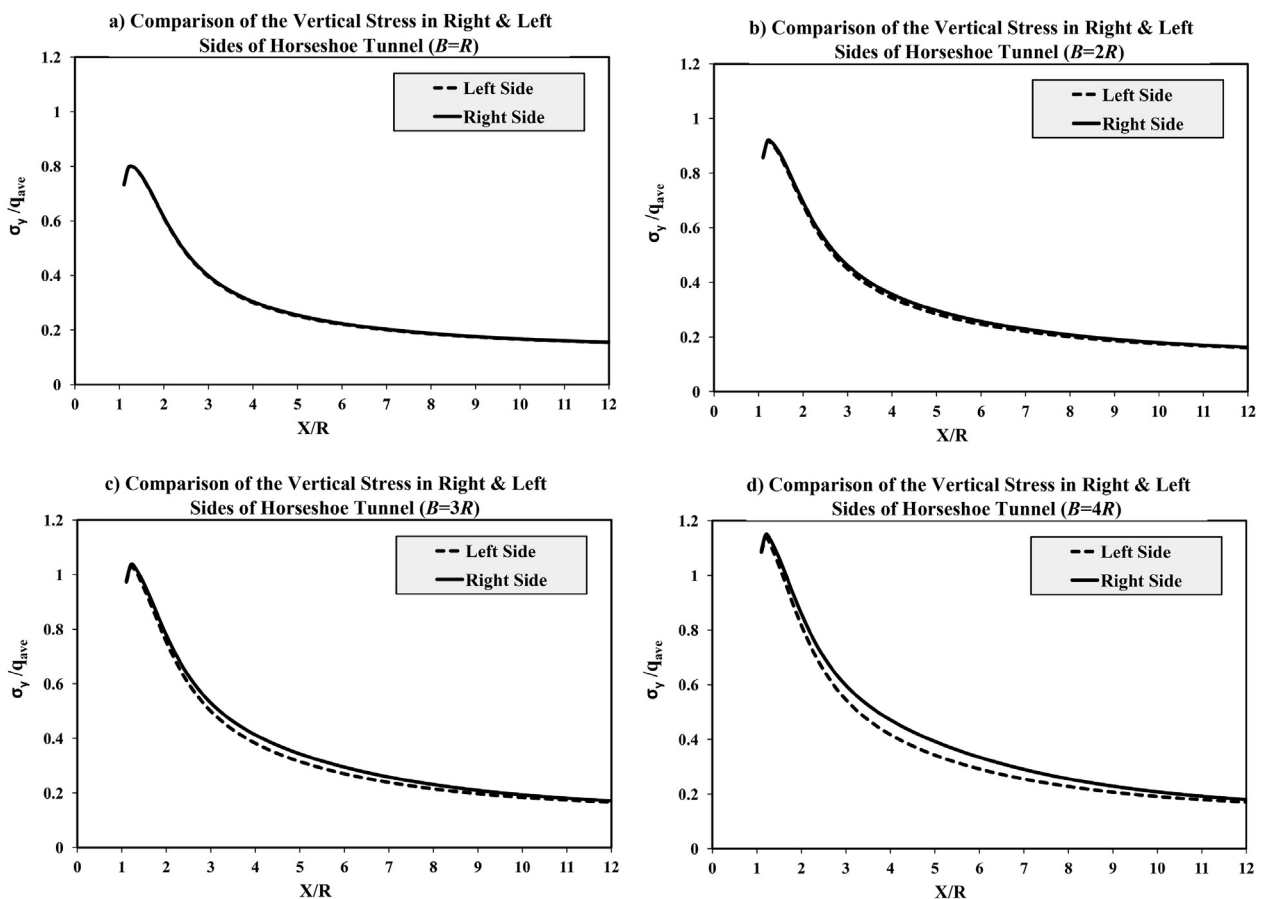

Fig. 13. Vertical stress in horizontal direction of tunnel wall in the left and right sides with the horseshoe section ($e = B/6$, $H/R = 8$, $D_f = R$, $q_{ave} = 200$ kPa).
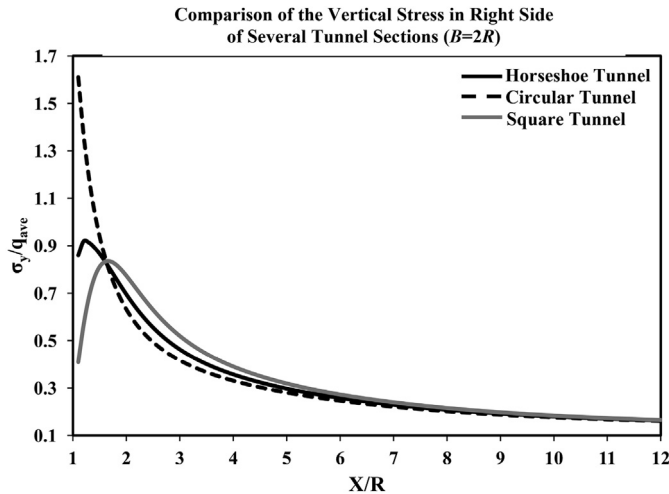
Fig. 14. Vertical stress in horizontal direction of tunnel wall with the circular, square, and horseshoe sections ($e = B/6$, $H/R = 8$, $D_f = R$, $q_{ave} = 200$ kPa, $B = 2R$).

and tunnel depth were considered as $D_f = R$ and $H = 8R$, respectively. Fig. 12 compares the vertical stress along the tunnel wall on the left/right sides for circular, square, and horseshoe tunnels (Fig. 11) with constant loading width ($B = 4R$). The results showed that the vertical stress on the right side of tunnel (having eccentricity) were higher than those on the left side; it is noteworthy that the two curves in each subfigure converged after a certain distance. Also, to show the vertical stress differences on the left and right sides, Fig. 13 is plotted for the tunnel with horseshoe cross-section. As can be seen, for the loading widths of $1R$ and $2R$, there was no significant difference between the left and right stress behaviors. As the loading width was increased, high stresses were obtained for the loading width of $2R$. By increasing loading width to $3R$ and $4R$, a significant change was observed between the right and left side stress behaviors because of the great influence of shallow loading eccentricity compared to that of the previous states. On the other hand, it was observed that the stress pattern was different around the horseshoe and square tunnels from that of the circular tunnel. In the circular case, no peak occurred. A comparative study is presented in Fig. 14. At the distances of less than $4R$, the difference between the patterns of tunnels with different cross-sections is obvious. It can be seen from Fig. 14 that the stress value always decreased with the distance from the tunnel and converges to a constant value due to the disappearing effect of underground opening.

Fig. 15 shows that, by increasing the loading width, the vertical stress was increased first for the circular, square and horseshoe tunnels. But, by increasing the distance from the tunnel wall, this difference disappeared and was converged to the gravity stress.

5. Conclusions

The favorable agreement of BEM results with the existing analytical solutions for the problem and the high accuracy of BEM confirmed that BEM can be used as a suitable method for modeling tunnels and the associated geotechnical structures. Parameters such as buried depth, tunnel cross-section, and eccentricity of shallow loading were studied. As was observed, these parameters can significantly influence the displacements and stresses around tunnels. Generally, the results of numerical modeling, failure condition, and induced stresses around the tunnel can be summarized as follows:
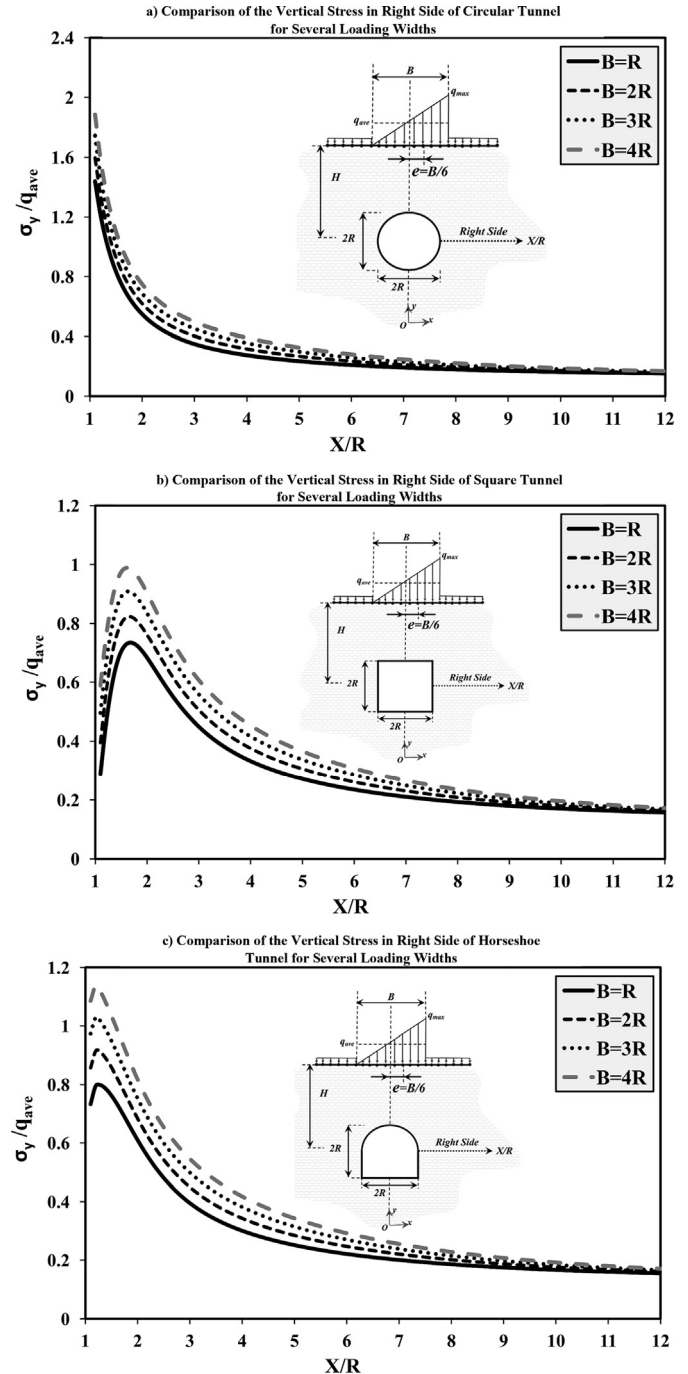

Fig. 15. Vertical stress along the horizontal direction of the tunnel wall with the circular, square, and horseshoe sections for different loading widths ($e = B/6$, $H/R = 8$, $D_f = R$, $q_{ave} = 200$ kPa).

(1) By increasing the width and eccentricity of shallow foundations, stress values as well as the failure radius around the tunnel are increased. It is noteworthy that the effects of this loading disappear from a specific depth and the tunnel behavior in a half-space would become similar to that in a full-space.

(2) By assuming fixed loading width ($B = 2R$), each tunnel section has a "minimum buried depth", at which the maximum failure radius occurs; if the tunnel is excavated below this minimum depth, it will collapse. For the tunnels with circular and horseshoe sections, the minimum buried depth is equal

to 6R ($H/R = 6$) and for those with square cross-sections, it is equal to 7R.

(3) By assuming fixed loading width ($B = 2R$), each tunnel section has an "optimum buried depth", at which the minimum failure radius occurs. At the depth less than or more than this value, due to the effects of shallow loading and gravity, failure radius would increase. Therefore, the optimum buried depth of circular and horseshoe tunnels is equal to 11R ($H/R = 11$), and for the tunnels with square cross-sections, it is equal to 12R ($H/R = 12$).

(4) From a specific buried depth, the effects of eccentricity disappear; this depth for the tunnel with a horseshoe cross-section and loading width of $B = 2R$ and 4R is equal to $H = 8R$ and 13R, respectively.

(5) The vertical stresses on the right side of the tunnel (having eccentricity) were higher than those on the left side and they converge after a certain distance.

(6) Stress behavior around the tunnels with horseshoe/square cross-sections is different from that of the circular tunnel, which can be attributed to the circle shape. On the other hand, by increasing the distance from the tunnel wall, the effect of loading width disappears and the stresses converge to the gravity stress.

Conflict of interest

The authors wish to confirm that there are no known conflicts of interest associated with this publication and there has been no significant financial support for this work that could have influenced its outcome.

References

Asgari Marnani J, Panji M. Behavior of strip footings on the clay soils under eccentric loading. Iranian Society of Civil Engineers Scientific Magazine (BANA) 2007;29:34–44.

Asgari Marnani J, Panji M. Boundary elements methods, theory and application. Newshanegar Pub.; 2008.

Atkinson JH, Cairncross AM. Collapse of a shallow tunnel in a Mohr–Coulomb material. In: Palmer AC, editor. Proceedings of the Symposium on the Role of Plasticity in Soil Mechanics. Cambridge, UK: University of Cambridge; 1973. p. 202–6.

Azevedo RF, Parreira AB, Zornberg JG. Numerical analysis of a tunnel in residual soils. Journal of Geotechnical and Geoenvironmental Engineering 2002;128(3):227–36.

Banerjee PK, Butterfield R. Boundary element methods in engineering science. 1st ed. London: McGraw-Hill; 1981.

Banerjee PK, Driscoll RM. Three-dimensional analysis of raked pile groups. Proceedings of the Institution of Civil Engineers 1976;61(4):653–71.

Benjumea R, Sikarskie DL. On the solution of plane orthotropic elasticity problems by an integral method. Journal of Applied Mechanics 1972;39(3):801–8.

Brebbia CA, Dominguez J. Boundary elements an introductory course. Southampton, UK: Computational Mechanics Publications; 1989.

Cairncross AM. Deformation around model tunnels in stiff clay [PhD Thesis]. Cambridge, UK: University of Cambridge; 1973.

Crouch SL, Starfield AM. Boundary elements methods in solid mechanics. Department of Civil and Mineral Engineering, University of Minnesota; 1983.

Davis EH, Gunn MJ, Mair RJ, Seneviratine HN. The stability of shallow tunnels and underground openings in cohesive material. Geotechnique 1980;30(4):397–416.

Fraldi M, Guarracino F. Analytical solutions for collapse mechanisms in tunnels with arbitrary cross sections. International Journal of Solids and Structures 2010;47(2):216–23.

Fraldi M, Guarracino F. Evaluation of impending collapse in circular tunnels by analytical and numerical approaches. Tunnelling and Underground Space Technology 2011;26(4):507–16.

Fraldi M, Guarracino F. Limit analysis of collapse mechanisms in cavities and tunnels according to the Hoek–Brown failure criterion. International Journal of Rock Mechanics and Mining Sciences 2009;46(4):665–73.

Fredholm I. Sur une classe d'équations fonctionelles. Acta Mathematica 1903;27(1):365–90 (in French).

Hoek E, Carranza-Torres C, Corkum B. Hoek-Brown failure criterion–2002 edition. In: Proc. NARMS-TAC Conference, Toronto, Canada; 2002. p. 267–73.

Hoek E, Marions PA. A brief history of the development of the Hoek-Brown failure criterion. Soils and Rocks 2007. http://www.rockscience.com/hoek/references.

Hoek E. Strength of jointed rock masses. Geotechnique 1983;33(3):187–223.

Jao M, Wang MC. Stability of strip footing above concrete-lined soft ground tunnels. Tunnelling and Underground Space Technology 1998;13(4):427–34.

Kooi CB, Verruijt A. Interaction of circular holes in an infinite elastic medium. Tunnelling and Underground Space Technology 2001;16(1):59–62.

Koutsabeloulis NC, Griffiths DV. Numerical modeling of the trap door problem. Geotechnique 1989;39(1):77–89.

Leca E, Dormieux L. Upper and lower bound solutions for the face stability of shallow circular tunnels in frictional material. Geotechnique 1990;40(4):581–606.

Lee KM, Rowe RK. An analysis of three-dimensional ground movements: the Thunder Bay Tunnel. Canadian Geotechnical Journal 1991;28(1):25–41.

Lyamin AV, Sloan SW. Stability of a plane strain circular tunnel in a cohesive frictional soil. In: Proceedings of the J.R. Booker Memorial Symposium. Rotterdam, Netherlands: A.A. Balkema; 2000. p. 139–53.

Mair RJ. Centrifugal modeling of tunnel construction in soft clay. PhD Thesis. Cambridge, UK: University of Cambridge; 1979.

Martin CD, Kaiser PK, McCreath DR. Hoek-Brown parameters for predicting the depth of brittle failure around tunnels. Canadian Geotechnical Journal 1999;36(1):136–51.

Massonnet CE. Numerical use of integral procedures. In: Zienkiewicz OC, Holister GS, editors. Stress analysis. John Wiley & Sons Inc.; 1965.

Muhlhaus HB. Lower bound solutions for circular tunnels in two and three dimensions. Rock Mechanics and Rock Engineering 1985;18(1):37–52.

Panji M, Asgari Marnani J, Alielahi H, Koohsari H, Adampira M. Evaluation of effective parameters on stress behavior of 2D shallow tunnels using boundary elements method. Journal of Transportation Research 2013;10(1):17–28.

Panji M, Asgari Marnani J, Tavousi Tafreshi Sh. Evaluation of effective parameters on the underground tunnel stability using BEM. Journal of Structural Engineering and Geotechnics 2011;1(2):29–37.

Panji M, Koohsari H, Adampira M. Effects of eccentric shallow loading on behavior of 2D tunnels. In: Dam and Tunnel Conference and Exposition. Tehran, Iran: Tehran University; 2012.

Panji M. Stress analysis of infinite and semi-infinite continuum media using BEM. MS Thesis. Central Tehran Branch: Islamic Azad University; 2007.

Park SH, Adachi T. Laboratory tests and FE analyses on tunneling in the unconsolidated ground with inclined layers. Tunnelling and Underground Space Technology 2002;17(2):181–93.

Poulos HG, Davis EH. Elastic solution for soil and rock mechanics. John Wiley & Sons Inc.; 1974.

Rowe RK, Kack GJ. A theoretical examination of the settlements induced by tunneling four case histories. Canadian Geotechnical Journal 1983;20(2):299–314.

Seneviratne HN. Deformations and pore-pressures around model tunnels in soft clay. PhD Thesis. Cambridge, UK: University of Cambridge; 1979.

Shah S. Practical implementation of the direct boundary element method for three-dimensional stress analysis of underground excavations. PhD Thesis. Department of Civil Engineering, University of Toronto; 1992.

Sloan SW, Assadi A. Stability of shallow tunnels in soft ground. In: Holsby GT, Schofield AN, editors. Predictive Soil Mechanics, Proceedings of the Wroth Memorial Symposium. London: Thomas Telford; 1993. p. 644–63.

Verruijt A. Deformations of an elastic half plane with a circular cavity. International Journal of Solids and Structures 1998;35(21):2795–804.

Yamamoto K, Lyamin AV, Wilson DW, Sloan SW, Abbo AJ. Bearing capacity of a cohesive-frictional soil with a shallow tunnel. In: Proceedings of the 13th Asian Regional Conference on Soil Mechanics and Geotechnical Engineering, Kolkata, India. New Delhi, India: Allied Publishers Pvt. Ltd.; 2012. p. 489–92.

Yamamoto K, Lyamin AV, Wilson DW, Sloan SW, Abbo AJ. Stability of a circular tunnel in cohesive-frictional soil subjected to surcharge loading. Computers and Geotechnics 2011a;38(4):504–14.

Yamamoto K, Lyamin AV, Wilson DW, Sloan SW, Abbo AJ. Stability of a single tunnel in cohesive-frictional soil subjected to surcharge loading. Canadian Geotechnical Journal 2011b;48(12):1841–54.

Yamamoto K, Lyamin AV, Wilson DW, Sloan SW, Abbo AJ. Stability of dual circular tunnels in cohesive-frictional soil subjected to surcharge loading. Computers and Geotechnics 2013;50:41–54.

Dr. **Mehdi Panji** is an Assistant Professor in the Department of Geotechnical Engineering, College of Technical and Engineering, Islamic Azad University of Zanjan (IAUZ). Dr. Panji has focused on the advanced numerical modeling in the geomechanics since 2007. In 2013, he holds a Ph.D. degree with honors in Geotechnical Earthquake Engineering from Islamic Azad University, Science and Research Branch, Tehran, Iran. His Ph.D. thesis was devoted to seismic analysis of topographic site effects subjected to propagating incident SH-waves by an approach called as direct half-plane time-domain BEM. He has developed general software known as DASBEM, which is able to conduct dynamic/static analysis of all geotechnical constructions with this method.